4. P. W. Shor, *Proceedings of the 35th Annual Symposium on Foundations of Computer Science* (IEEE Computer Society Press, Los Alaminos, CA 1994), pp. 124–134.
5. C. H. Bennett, P. W. Shor, *Science* **303**, 1784 (2004).
6. B. Schumacher, M. A. Nielsen, *Phys. Rev. A* **54**, 2629 (1996).
7. W. Wootters, W. Zurek, *Nature* **299**, 802 (1982).
8. S. Lloyd, *Phys. Rev. A* **55**, 1613 (1997).
9. P. W. Shor, lecture notes from the Mathematical Sciences Research Institute Workshop on Quantum Computation, Berkeley, CA, 2002. Available online at www.msri.org/publications/ln/msri/2002/quantumcrypto/shor/1/.
10. I. Devetak, *IEEE Trans. Inf. Theory* **51**, 44 (2005).
11. D. DiVincenzo, P. W. Shor, J. A. Smolin, *Phys. Rev. A* **57**, 830 (1998).
12. G. Smith, J. A. Smolin, *Phys. Rev. Lett.* **98**, 030501 (2007).
13. C. H. Bennett, D. P. DiVincenzo, J. A. Smolin, *Phys. Rev. Lett.* **78**, 3217 (1997).
14. M. Horodecki, P. Horodecki, R. Horodecki, *Phys. Lett. A* **223**, 1 (1996).
15. P. Horodecki, *Phys. Lett. A* **232**, 333 (1997).
16. A. Peres, *Phys. Rev. Lett.* **77**, 1413 (1996).
17. G. Smith, J. Smolin, A. Winter, *IEEE Trans. Inf. Theory* **54**, 4208 (2008).
18. K. Horodecki, M. Horodecki, P. Horodecki, J. Oppenheim, *Phys. Rev. Lett.* **94**, 160502 (2005).
19. K. Horodecki, L. Pankowski, M. Horodecki, P. Horodecki, *IEEE Trans. Inf. Theory* **54**, 2621 (2008).
20. Further details can be found in the supporting online material on *Science* Online.
21. P. Shor, J. Smolin, A. Thapliyal, *Phys. Rev. Lett.* **90**, 107901 (2003).
22. W. Dur, J. Cirac, P. Horodecki, *Phys. Rev. Lett.* **93**, 020503 (2004).
23. R. Duan, Y. Shi, *Phys. Rev. Lett.* **101**, 020501 (2008).
24. L. Czekaj, P. Horodecki, preprint available at http://arxiv.org/pdf/0807.3977.
25. P. Horodecki, M. Horodecki, R. Horodecki, *Phys. Rev. Lett.* **82**, 1056 (1999).
26. P. Shor, J. Smolin, B. Terhal, *Phys. Rev. Lett.* **86**, 2681 (2001).

27. We are indebted to C. Bennett, C. Callaway, E. Timmermans, B. Toner, and A. Winter for encouragement and comments on an earlier draft. J.Y. is supported by the CNLS and the Quantum Institute through grants provided by the Laboratory Directed Research and Development program of the U.S. Department of Energy.

Supporting Online Material

www.sciencemag.org/cgi/content/full/1162242/DC1
SOM Text
References

24 June 2008; accepted 13 August 2008
Published online 21 August 2008;
10.1126/science.1162242
Include this information when citing this paper.

Synthesis and Solid-State NMR Structural Characterization of ^{13}C-Labeled Graphite Oxide

Weiwei Cai,[1,2] Richard D. Piner,[1] Frank J. Stadermann,[3] Sungjin Park,[1] Medhat A. Shaibat,[4] Yoshitaka Ishii,[4] Dongxing Yang,[1] Aruna Velamakanni,[1] Sung Jin An,[5] Meryl Stoller,[1] Jinho An,[1] Dongmin Chen,[2] Rodney S. Ruoff[1]*

The detailed chemical structure of graphite oxide (GO), a layered material prepared from graphite almost 150 years ago and a precursor to chemically modified graphenes, has not been previously resolved because of the pseudo-random chemical functionalization of each layer, as well as variations in exact composition. Carbon-13 (^{13}C) solid-state nuclear magnetic resonance (SSNMR) spectra of GO for natural abundance ^{13}C have poor signal-to-noise ratios. Approximately 100% ^{13}C-labeled graphite was made and converted to ^{13}C-labeled GO, and ^{13}C SSNMR was used to reveal details of the chemical bonding network, including the chemical groups and their connections. Carbon-13–labeled graphite can be used to prepare chemically modified graphenes for ^{13}C SSNMR analysis with enhanced sensitivity and for fundamental studies of ^{13}C-labeled graphite and graphene.

Unlike crystalline materials, the structure of materials that are amorphous or that vary in chemical composition can be difficult to determine. Solid-state nuclear magnetic resonance (SSNMR) can provide important structural insights, but often requires very high enrichment of nuclei with NMR-active spins. One example of such a material that has proven difficult to characterize, despite having been first prepared almost 150 years ago (*1*), is graphite oxide (GO), which can be prepared by heating graphite in oxidizing chemicals. GO is a layered material containing interlamellar water. Materials derived from GO include its chemically functionalized (*2*), reduced (*3*), and thermally expanded forms (*4*), as well as chemically modified graphenes (*2*, *3*, *5*–*8*).

SSNMR has been done on GO but has not provided a complete understanding of the chemical structure of this material, although the detailed chemical structure has been actively researched for many years (*2*, *7*). One difficulty is that the spectra do not attain a high signal-to-noise (S/N) ratio for natural abundance ^{13}C. The lack of ^{13}C-labeled GO has prevented application of modern multidimensional SSNMR methods that can provide information on the bonding arrangements of atoms and their connectivities. Although a series of one-dimensional (1D) ^{13}C SSNMR studies for GO and reduced GO revealed signal assignments and the basic chemical compositions of each, there is sparse experimental evidence of the connectivities of the chemical groups such as sp^2-bonded carbons (C=C), epoxide, carbonyl, and carboxylic groups. Thus, a variety of structural models of GO are still debated (*2*). However, we found from Monte Carlo simulations that even at only 20% ^{13}C, the abundance of ^{13}C-^{13}C bonds will be 400 times that of an unlabeled sample, so that the time required for detecting ^{13}C-^{13}C pairs in SSNMR of such a

[1]Department of Mechanical Engineering and the Texas Materials Institute, University of Texas at Austin, Austin, TX 78712, USA. [2]Beijing National Laboratory for Condensed Matter Physics, Institute of Physics, Chinese Academy of Sciences, Beijing 100080, China. [3]Laboratory for Space Sciences, Department of Physics, Washington University, St. Louis, MO 63130, USA. [4]Department of Chemistry, University of Illinois at Chicago, 845 West Taylor Street, Chicago, IL 60607, USA. [5]National Creative Research Initiative Center for Semiconductor Nanorods and Department of Materials Science and Engineering, Pohang University of Science and Technology, Pohang, Gyeongbuk 790-784, Korea.

*To whom correspondence should be addressed. E-mail: r.ruoff@mail.utexas.edu

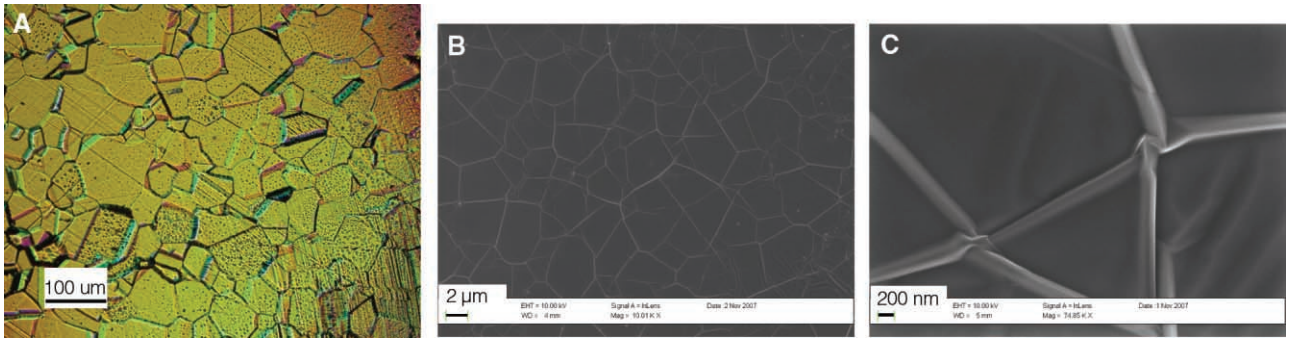

Fig. 1. (**A**) Optical images of Ni, and SEM images of (**B**) ^{13}C-labeled synthetic graphite and (**C**) the wrinkles.

sample will be less by a factor of about 160,000 than that of unlabeled samples. Evaluation of detailed bonding networks (three neighboring ^{13}C's and so on) can be done with Monte Carlo modeling in a straightforward way for any percentage labeling of ^{13}C.

There have been a number of recent publications exploring the catalytic growth of graphite or graphitic structures (*9*–*20*). We have developed a thermal chemical vapor deposition (CVD) method for growing synthetic graphite from methane on a resistively heated Ni foil as a catalytic substrate.

A detailed description of our reactor is given in the supporting online material (*21*). Briefly, our reactor consists of a vacuum chamber with a metal foil supported in the center with high-current electrodes. The Ni foil can be resistively heated to near its melting point. During the deposition, the substrate temperature was held at ~1200° to 1300°C and the pressure at 1 atm. The gas used was a mixture of 10% methane and 90% Ar. The methane was 1%, 30%, 50%, 70%, and 99.95% $^{13}CH_4$, in different growth runs. A deposition rate of ~2 μm/hour (for thin films) was obtained, and the growth rate was slowed to ~0.2 μm/hour for thicker films. Atomic force microscopy (AFM), scanning electron microscopy (SEM), x-ray diffraction (XRD), and Raman spectroscopy confirmed that the as-deposited carbon was very high-quality graphite. The graphite films deposited onto the Ni foils appeared very smooth and continuous by optical microscopy (Fig. 1). The smooth surface areas are separated from each other by wrinkles that are likely caused by the different thermal expansion coefficients of the deposited graphite and the nickel substrate (*17*). A typical smooth surface region is about 2 μm across, much smaller than the substrate grain sizes, and the typical wrinkle height as obtained by AFM is about 50 nm (fig. S2) (*21*). The ^{13}C content of the graphite samples was measured with a modified CAMECA ims3f secondary ion mass spectrometry (SIMS) instrument (CAMECA, Gennevilliers, France). The analytical error of these measurements is estimated to be ~5%, largely because the sample surfaces are uneven on a 10 to 100 μm scale. The ^{13}C content of each of the graphite films measured by SIMS was 1%, 19%, 41%, 54%, and 86% for samples prepared from 1%, 30%, 50%, 70%, and 99.95% $^{13}CH_4$, respectively. The ^{13}C contents measured by SIMS (19%, 41%, 54%, and 86%) differed significantly from the percentages of $^{13}CH_4$ used because for these four experimental runs the chamber had accumulated considerable residual carbon-containing material from many trial experiments with unlabeled methane. A thorough cleaning of the chamber before another run with 99.95% $^{13}CH_4$ yielded 99.5% ^{13}C-content synthetic graphite measured by SIMS. Use of a clean chamber is thus important for the ^{13}C content of the graphite to more closely match the ^{13}C content of the input $^{13}CH_4$ and $^{12}CH_4$.

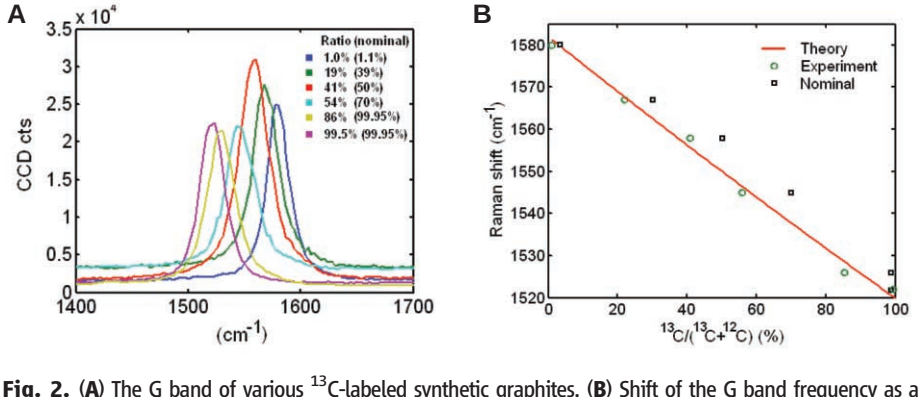

Fig. 2. (**A**) The G band of various ^{13}C-labeled synthetic graphites. (**B**) Shift of the G band frequency as a function of percentage of ^{13}C, as determined by SIMS. The theoretical curve was obtained as described in (*21*).

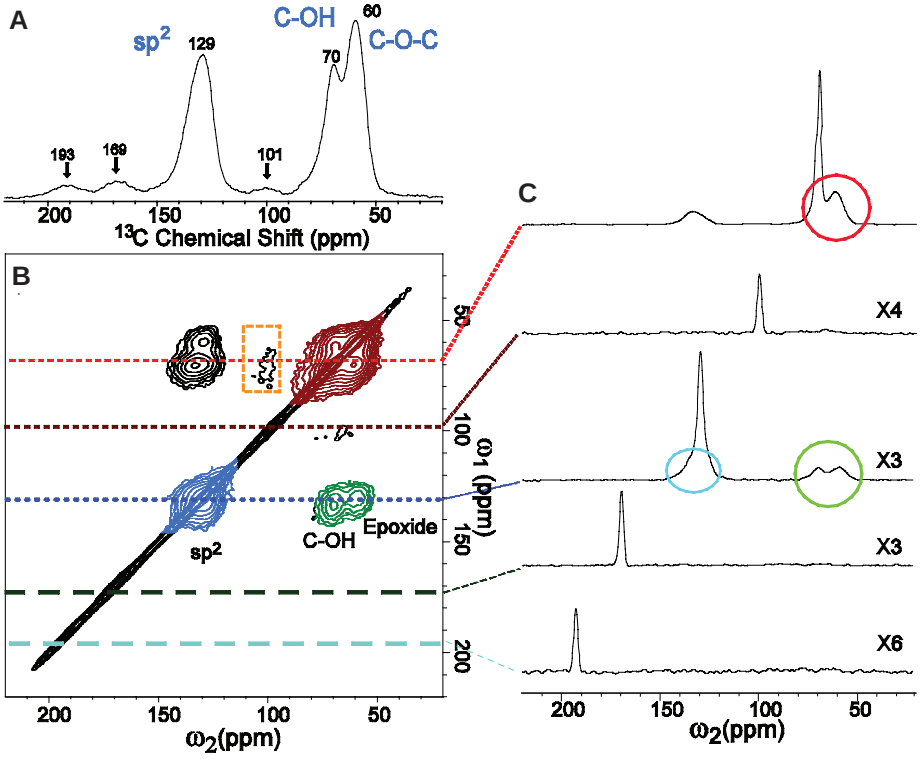

Fig. 3 (**A**) 1D ^{13}C MAS and (**B**) 2D $^{13}C/^{13}C$ chemical-shift correlation solid-state NMR spectra of ^{13}C-labeled graphite oxide with (**C**) slices selected from the 2D spectrum at the indicated positions (70, 101, 130, 169, and 193 ppm) in the ω_1 dimension. All the spectra were obtained at a ^{13}C NMR frequency of 100.643 MHz with 90 kHz ^1H decoupling and 20 kHz MAS for 12 mg of the sample. In (A), the ^{13}C MAS spectrum was obtained with direct ^{13}C excitation by a $\pi/2$-pulse. The recycle delay was 180 s, and the experimental time was 96 min for 32 scans. In (B), the 2D spectrum was obtained with cross polarization and fpRFDR ^{13}C-^{13}C dipolar recoupling sequence (*24*). The experimental time is 12.9 hours with recycle delays of 1.5 s and 64 scans for each real or imaginary t_1 point. A Gaussian broadening of 150 Hz was applied. The green, red, and blue areas in (B) and circles in (C) represent cross peaks between sp^2 and C-OH/epoxide (green), those between C-OH and epoxide (red), and those within sp^2 groups (blue), respectively.

Raman spectra were acquired and the peak frequency shifts caused by ^{13}C-enrichment were determined. Figure 2 shows the relationship between the wave number of the G band and the $^{13}C/^{12}C$ ratio. The Raman frequencies shift from 1580 cm^{-1} to 1523 cm^{-1}, from unlabeled to 99.5% ^{13}C graphite (as measured by SIMS), respectively. There is good agreement between the frequency shift and the square root of the atomic mass, assuming the respective bond force constants.

AFM, SEM, and XRD data, as well as further details about SIMS and Raman analysis of ^{13}C-labeled graphite, are presented in (*21*).

High-resolution SSNMR using magic angle spinning (MAS) has been used as a primary method to characterize GO at the molecular level (*2*, *22*, *23*). Figure 3A shows 1D ^{13}C MAS spectrum, and Fig. 3B shows 2D $^{13}C/^{13}C$ chemical-shift correlation SSNMR spectrum of ^{13}C-labeled GO (made from approximately 100% ^{13}C-labeled graphite) that was prepared using a modified Hummer's method (*2*) with ^{13}C-labeled graphite (*21*). The signal assignments for the three major

peaks at 59.7 (epoxide ^{13}C), 69.6 (^{13}C-OH), and 129.3 (sp^2 ^{13}C) parts per million (ppm) in Fig. 3A are based on studies by Lerf *et al*. (*23*). We performed additional analyses and confirmed that these assignments are likely correct (*21*). The obtained 1D spectrum shows similar features with those reported in (*23*) except for the relatively well-resolved minor peaks at 101, 169, and 193 ppm, which respectively yield only 12%, 15%, and 4% of the integrated intensity of the 70-ppm peak. The spectrum shows a considerably stronger sp^2 peak and a much weaker peak at 169 ppm compared with that by Szabo *et al*. (*22*), although the observed peak positions are similar. The peak at 169 ppm was previously attributed to ^{13}C=O (*22*). The results imply that their sample was subject to a higher level of oxidization than ours.

Because the natural abundance of ^{13}C is only 1%, attaining sufficient sensitivity in a 2D spectrum, as shown in Fig. 3B, is extremely difficult without the ^{13}C-labeled samples. For example, ^{13}C-^{13}C bonds exist only at 0.01% abundance without labeling; thus, obtaining an equivalent 2D spectrum for an unlabeled sample would require about 10^8 times as much time. The experiment in Fig. 3B was performed with a finite-pulse radio frequency–driven dipolar recoupling (fpRFDR) mixing sequence (*24*). With the labeled sample and a relatively short mixing time (1.6 ms), the experiment permitted us to identify ^{13}C-^{13}C pairs directly bonded or separated by two bonds. In Fig. 3B, there are several strong cross peaks. For example, cross peaks were observed at the positions (ω_1, ω_2) = (133 ppm, 70 ppm) and (130 ppm, 59 ppm) (green signals in Fig. 3B). These cross peaks represent spin polarization transfer from sp^2 carbons observed at ~130 ppm in ω_1, to C-OH and epoxide groups, which appear at 70 ppm and 59 ppm in ω_2, respectively. Unlike previous studies, these cross peaks directly present the connectivity between sp^2 ^{13}C and ^{13}C-OH, as well as that between sp^2 and epoxide ^{13}C through spin-spin dipolar couplings. The cross peak intensities are about 10%, compared with the diagonal signals, which represent signals for ^{13}C spins that had the same NMR frequencies in the two dimensions ($\omega_1 = \omega_2$). The relatively strong intensities of the cross peaks suggest that a large fraction of the sp^2 ^{13}C atoms are directly bonded to ^{13}C-OH and/or epoxide ^{13}C.

We also observed strong cross peaks between ^{13}C-OH and ^{13}C-epoxide (red signals). Again, the data suggest that a large fraction of C-OH and epoxide carbons are bonded to each other. The blue cross peaks indicate that there are sp^2 species having slightly different chemical shifts and that they are bonded with each other. Indeed, the sp^2 ^{13}C shifts for the cross peaks (green) are slightly different for the cross peaks to C-OH (133 ppm) and that to epoxide (130 ppm).

In the previous studies (*23*), the proximities of the chemical groups were tentatively assigned based on formation of the phenol group during the deoxidization of GO. In contrast, the present SSNMR data directly shows that these groups are chemically bonded. For the minor species, we found cross peaks only for the peak at 101 ppm (orange box). There are no visible cross peaks for the other minor components at 169 and 193 ppm, despite these minor peaks having comparable intensities to the 101-ppm peak. The results imply that these minor components at 169 and 193 ppm, which were previously attributed to the presence of C=O (*2*, *22*), are spatially separated from a majority of the sp^2, C-OH, and epoxide carbons.

Among six previously proposed models (*22*), only two, the Lerf-Klinowski model (*23*) and the Dékány model (*22*), present such a network. The model proposed by Dékány *et al*. may be correct for their more highly oxidized compound, because that structural model seems to call for a considerably higher level of oxidization to complete the modification of an sp^2 network into a network of linked cyclohexanes. Further studies would be needed to define all of the structural details of the system.

Chemically modified graphenes that will be of importance in a variety of new materials can now be ^{13}C-labeled and more effectively studied by SSNMR. High-quality ^{13}C-labeled graphite should find use for fundamental property measurements, including of ^{13}C-labeled graphene.

References and Notes

1. B. C. Brodie, *Annales des Chimie et des Physique* **59**, 466 (1860).
2. S. Stankovich *et al*., *Carbon* **45**, 1558 (2007).
3. S. Stankovich *et al*., *J. Mater. Chem.* **16**, 155 (2006).
4. M. J. McAllister *et al*., *Chem. Mater.* **19**, 4396 (2007).
5. D. A. Dikin *et al*., *Nature* **448**, 457 (2007).
6. S. Stankovich *et al*., *Nature* **442**, 282 (2006).
7. S. Stankovich, R. D. Piner, S. T. Nguyen, R. S. Ruoff, *Carbon* **44**, 3342 (2006).
8. S. Watcharotone *et al*., *Nano Lett.* **7**, 1888 (2007).
9. H. H. Angermann, G. Horz, *Appl. Surf. Sci.* **70-71**, 163 (1993).
10. R. Anton, *J. Mater. Res.* **20**, 1837 (2005).
11. A. Barbangelo, R. Sangiorgi, *Mater. Sci. Eng. A* **156**, 217 (1992).
12. F. Bonnet, F. Ropital, Y. Berthier, P. Marcus, *Mater. Corrosion Werkst. Korros.* **54**, 870 (2003).
13. D. V. Fedoseev, S. P. Vnukov, B. V. Derjaguin, *Carbon* **17**, 453 (1979).
14. D. Fujita, T. Homma, *Surf. Interface Anal.* **19**, 430 (1992).
15. D. Fujita, K. Yoshihara, *J. Vac. Sci. Technol. A* **12**, 2134 (1994).
16. C. Klink, I. Stensgaard, F. Besenbacher, E. Laegsgaard, *Surf. Sci.* **342**, 250 (1995).
17. A. N. Obraztsov, E. A. Obraztsova, A. V. Tyurnina, A. A. Zolotukhin, *Carbon* **45**, 2017 (2007).
18. H. Oudghiri-Hassani, S. Rakass, N. Abatzoglou, P. Rowntree, *J. Power Sources* **171**, 850 (2007).
19. R. Sinclair, T. Itoh, R. Chin, *Microsc. Microanal.* **8**, 288 (2002).
20. M. Yudasaka, R. Kikuchi, Y. Ohki, S. Yoshimura, *J. Vac. Sci. Technol. A* **16**, 2463 (1998).
21. Materials and methods are available as supporting material on *Science* Online.
22. T. Szabo *et al*., *Chem. Mater.* **18**, 2740 (2006).
23. A. Lerf, H. Y. He, M. Forster, J. Klinowski, *J. Phys. Chem. B* **102**, 4477 (1998).
24. Y. Ishii, *J. Chem. Phys.* **114**, 8473 (2001).

25. $^{13}CH_4$ was provided through a research grant from Cambridge Isotopes Laboratories, Inc. We (R.S.R.) wish to acknowledge The University of Texas for startup funds and for partial support by the *Defense Advanced Research Projects Agency* Center on Nanoscale Science and Technology for Integrated Micro/NanoElectromechanical Transducers (HR0011-06-1-0048). The WiTec Micro-Raman instrument was acquired by an Air Force Office of Scientific Research, Defense University Research Instrumentation Program grant. Y.I. appreciates support from the Dreyfus Foundation Teacher-Scholar Award program and the NSF CAREER program (CHE 449952). S.J.A. was financially supported by the Korea Science and Engineering Foundation under the National Creative Research Initiative Project (R16-2004-004-01001-0) of the Ministry of Science and Technology, Korea. J. Goodenough and A. Ruoff commented on an early version of this manuscript.

Supporting Online Material

www.sciencemag.org/cgi/content/full/321/5897/1815/DC1
Materials and Methods
Figs. S1 to S5
References

26 June 2008; accepted 15 August 2008
10.1126/science.1162369

Linear Response Breakdown in Solvation Dynamics Induced by Atomic Electron-Transfer Reactions

Arthur E. Bragg, Molly C. Cavanagh, Benjamin J. Schwartz*

The linear response (LR) approximation, which predicts identical relaxation rates from all nonequilibrium initial conditions that relax to the same equilibrium state, underlies dominant models of how solvation influences chemical reactivity. We experimentally tested the validity of LR for the solvation that accompanies partial electron transfer to and from a monatomic solute in solution. We photochemically prepared the species with stoichiometry Na^0 in liquid tetrahydrofuran by both adding an electron to Na^+ and removing an electron from Na^-. Because atoms lack nuclear degrees of freedom, ultrafast changes in the Na^0 absorption spectrum reflected the solvation that began from our two initial nonequilibrium conditions. We found that the solvation of Na^0 occurs more rapidly from Na^+ than Na^-, constituting a breakdown of LR. This indicates that Marcus theory would fail to describe electron-transfer processes for this and related chemical systems.

Solvent-solute interactions play an integral role in solution-phase chemical reactivity and particularly in electron-transfer (ET) reactions (*1*), in which solvation dynamics—the response of the solvent to changes in solute size and/or electronic charge distribution (*2*)—help drive the motion of charge from donor to acceptor. Current theoretical understanding of how